Physics Letters A ••• (••••) •••–•••

Contents lists available at ScienceDirect

Physics Letters A

www.elsevier.com/locate/pla

Effect of strain on electronic and magnetic properties of Fe-doped monolayer SnS_2

Yaming Liu [a], Fei Wang [b], Dechuan Kong [a], Bo Hu [a], Congxin Xia [c], Jianxiu Su [a]

[a] *Henan Institute of Science and Technology, Xinxiang 453003, China*
[b] *School of Physics and Engineering, Zhengzhou University, Zhengzhou 450001, China*
[c] *Henan Normal University, Xinxiang 453003, China*

ARTICLE INFO

Article history:
Received 5 January 2017
Received in revised form 1 March 2017
Accepted 17 March 2017
Available online xxxx
Communicated by M. Wu

Keywords:
Fe-doped SnS_2
Monolayer
DFT
Strain

ABSTRACT

Using the first-principles calculation, the electronic and magnetic properties of Fe-doped SnS_2 monolayer are investigated considering compressive and tensile biaxial strains. The optimized structures and formation energies indicate that the easily exfoliated monolayer from different bulk phase have the same configuration. Numerical results show that Fe-doped SnS_2 monolayer is half-metal and more energetically stable under the S-rich environment. Moreover, the induced magnetic moment is $1.986\mu_B$/atom. Compressive strain up to −6% or even more leads to a transformation from half-metal to semiconductor, while tensile strain makes the Fe-doped compound changing into a metal before the yielding point +15%, where a serious structural deformation appears. In particular, total magnetic moments are robust under the affordable biaxial strain.

1. Introduction

Nowadays, due to the extensive and potential applications in nanoelectronic and photovoltaic devices, considerable and intensive interests have been focused on the two-dimensional (2D) layered materials [1,2]. Among these compounds, 2D tin disulfide (SnS_2) is attracting much more attention for the proper wide band gap ~2.0 eV [3,4], high optical absorption coefficient $>10^4$ cm^{-1} in visible range [5], peculiar layered crystal structure [6], higher capacity [7], earth-abundant and environmentally friendly properties [8]. These advantages indicate that 2D SnS_2 can be a good candidate for window material in thin film solar cells, visible light sensitive photocatalyst and used as anode material for lithium-ion batteries, etc. Furthermore, compared with bulk SnS_2 counterpart, 2D nanostructures (such as nanoparticle, nanoplate, nanosheet) especially monolayer SnS_2 exhibit more preeminent properties due to quantum size confinement effect associated to the ultrathin structure. By refluxing parent bulk SnS_2 in formamide, Y. Sun et al. firstly synthesized the freestanding SnS_2 single layer of three atom thickness through a liquid exfoliation strategy, and experimentally confirmed that monolayer SnS_2 can be a good photocatalyst for visible-light water splitting [9]. Combining ultrathin SnS_2 nanosheets with graphene, Chang et al. demonstrated that the hybrid shows extraordinary Li^+ storage capacity and excellent cycling stability [10].

On the other hand, previous studies have showed that 2D SnS_2 possesses the nonmagnetic ground state [8,11], and the characteristic of magnetism always plays an important role in 2D semiconductor-based spintronics devices. Thus, dopant atoms are used to induce and manipulate magnetism in 2D SnS_2 and have caught the extensive attention by providing a new platform to explore novel functionalities. G. Kiruthigaa et al. synthesized Zn- and Ce-doped SnS_2, and found the photocatalytic activity was enhanced [12,13]. Doped with V or W ions, the ternary alloys were reported as promising intermediate band absorber materials in photovoltaic devices [14]. Replacing sulfur atoms with group V-, VII-elements, Xia et al. systematically studied the n- and p-type dopants in SnS_2 nanosheets [15]. Alqarni et al. prepared Fe-doped nanoflakes and reported the excellent optical properties [16]. Sun et al. theoretically studied the magnetic and optical properties of Fe-doped bulk SnS_2 [17,18], and found that with increasing the Fe-doped concentrations up to 12.5%, the adsorption coefficient in visible region increases monotonically. However, to the best of our knowledge, few works have been done on the Fe-doped monolayer SnS_2, especially the effect of strain on this compound. A better theoretical characterization of Fe-doped monolayer SnS_2 nanosheet would allow for better understanding in the mentioned practical applications and provide helpful supplementary for experiments. As reported before [19], strain represents an important challenge

E-mail address: amynliou@163.com (Y. Liu).

http://dx.doi.org/10.1016/j.physleta.2017.03.034
0375-9601/

in integrated circuits and devices, due to the mismatched lattice parameters and different coefficients of thermal expansion. Also, the role of strain is an effective way to induce and control the electronic and magnetic properties of materials, and is critical for rational device design. Here, in this paper, structural, electronic and magnetic properties, and the biaxial strain effect of Fe-doped SnS_2 monolayers were explored using first-principles calculations. Our results show that the Fe dopant can be energetically stable, and electronic structures can be turned effectively by biaxial strain, while the induced magnetic moments are robust. These results may clarify the Fe-doped effect in SnS_2, and would further stimulate the exploration of doping in SnS_2 for improved performance in nanodevices.

2. Computational methods

All the performed calculations in this work were based on the density functional theory as implemented in VASP [20,21]. The exchange and correlation interactions were described in the Perdew–Burke–Ernzerhofer (PBE) version of the GGA [22,23]. The wave-functions were expressed by projector augmented-wave (PAW) method and a kinetic energy cutoff of 400 eV was selected to ensure the convergence [24]. The *k*-mesh sampling used the Monkhorst–Pack scheme [25]. To obtain more exact band gaps, the on-site Coulomb repulsion and exchange interaction was introduced to describe the *d* electronic states [26]. The effective *U* was chosen 9.0 eV and 1.7 eV for Sn-4*d* and Fe-3*d* electrons respectively. SnS_2 adopts a peculiar layered crystal structure, the weak van der Waals interactions between layers of bulk were described in Grimme's DFT-D2 method [27]. For the single-layer calculations, a $4 \times 4 \times 1$ supercell with vacuum of 15 Å was used.

3. Results and discussion

3.1. Structural and electronic configurations of bulk and monolayer SnS_2

SnS_2 is a semiconductor and has a class of compounds with the CdI_2-type crystal structure. The most significant and widely studied configurations are the 2H- and 4H-type (H- for hexagonal), see Fig. 1(a) and (b). Sandwiching tin cations into two layers of sulfur atoms, the strongly bonded S–Sn–S triple-layer can be treated as basic structural unit, and is connected together by weak van der Waals interaction. The perpendicular stacking arrangements of the triple-layer along *c*-axis contributed to the different polytypes. 2H-type is the simplest structure with one molecular unit per unit cell (space group P-3m1, No. 164). In the 4H-polytype ($P6_3mc$, No. 186), a half-bond displacement of the second triple-layer occurs in the *ab*-plane. Thus, the lattice constant *a* is the same, while *c* approximately doubled with respect to the 2H-type. Whichever the parent bulk compounds, the exfoliated single triple-layer unit, *i.e.* monolayer nanosheet, has the same structural configuration with space group P-3m1. In SnS_2, each Sn ion coordinates to 6 S ions in a regular octahedral.

The lattice parameters of bulk and monolayer SnS_2 calculated by DFT are listed in Table 1, and compared with previous theoretical and experimental data. The PBE overestimated the lattice constants *a* and *c* of bulk 2H- (4H-) by 2.1% (1.8%), and 15.8% (16.1%), respectively. In contrast, Grimme method provides an excellent description of the crystal structure with an average error less than 2%. We found that the influences of van der Waals interaction are much more obvious on *c* than *a* of bulk phase SnS_2. Due to the reduction of dimensionality from 3D-bulk to 2D-monolayer, an obvious structure relaxation is expected for the absence of van der Waals interlayer interaction in monolayer configuration. The fully relaxed monolayer configuration appears to be planar structure, and the in-plane lattice parameters are a little bigger about ∼1% than that of the bulk phases.

It can clearly be seen from Fig. 2 that both 2H- and 4H- bulk phase SnS_2 crystals possess an indirect band gap, with the valence band maximum (VBM) locates along Γ–M, and very close to Γ point. In addition, the conduction band minimum (CBM) lies

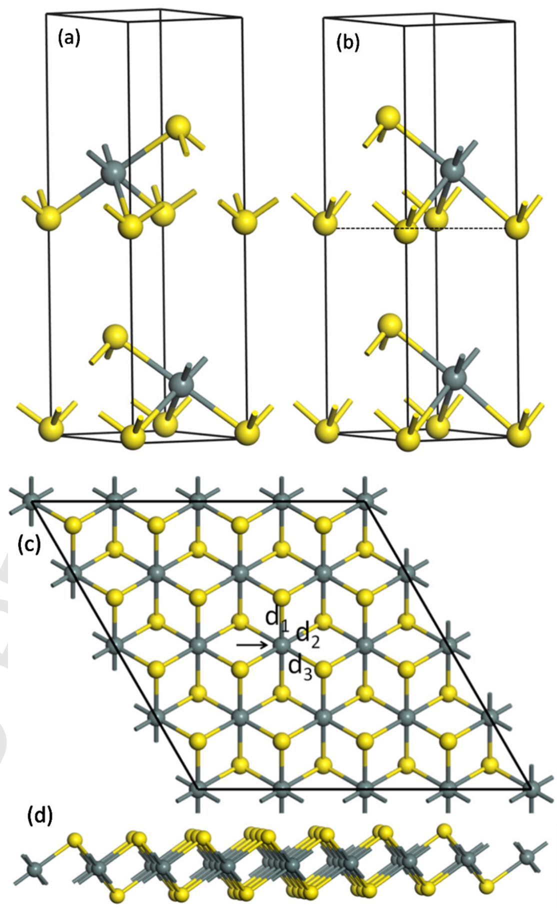

Fig. 1. Schematics of SnS_2 in different structures. (a) 4H-type ($P6_3mc$), (b) $1 \times 1 \times 2$ supercell of 2H-type (P-3m1), the horizontal dashed line is used to separate the figure into two primitive cells of 2H-SnS_2 configuration, (c) top and (d) side view of 4×4 supercell of monolayer SnS_2, the central Sn atom marked with a black arrow will be replaced by a Fe in the next text. Gray and yellow spheres represent the Sn and S atoms. (For interpretation of the references to color in this figure legend, the reader is referred to the web version of this article.)

Table 1
Lattice constants, S–Sn bond lengths d_{S-Sn} and band gaps E_g of SnS_2 in different crystal structures calculated with different DFT frameworks, and compared with previous theoretical and experimental reports.

	2H		4H		Monolayer	
	DFT-D2 (PBE)	Reference	DFT-D2 (PBE)	Reference	PBE	Reference
a (Å)	3.573 (3.701)	3.518 [8]; 3.649 [28]	3.581 (3.700)	3.648 [29]; 3.645 [15]	3.689	3.700 [9]
c (Å)	6.159 (6.774)	5.844 [8]; 5.899 [28]	11.695 (13.710)	11.802 [29]; 11.80 [15]	–	–
d_{S-Sn} (Å)	2.485 (2.596)	2.467 [8]	2.485 (2.678)	2.57 [15]	2.591	2.600 [9]
E_g (eV)	2.141 (1.660)	1.926 [8]	1.775 (1.425)	2.000 [9]; 1.482 [15]	1.650	1.587 [15]

Please cite this article in press as: Y. Liu et al., Effect of strain on electronic and magnetic properties of Fe-doped monolayer SnS_2, Phys. Lett. A (2017), http://dx.doi.org/10.1016/j.physleta.2017.03.034